Enhancing phonon transmission across a Si/Ge interface by atomic roughness: First-principles study with the Green's function method

Zhiting Tian, Keivan Esfarjani, and Gang Chen*

Department of Mechanical Engineering, Massachusetts Institute of Technology, Cambridge, Massachusetts 02139, USA

(Received 23 August 2012; published 10 December 2012)

Knowledge on phonon transmittance as a function of phonon frequency and incidence angle at interfaces is vital for multiscale modeling of heat transport in nanostructured materials. Although thermal conductivity reduction in nanostructured materials can usually be described by phonon scattering due to interface roughness, we show how a Green's function method in conjunction with the Landauer formalism suggests that interface roughness induced by atomic mixing can increase phonon transmission and interfacial thermal conductance. This is an attempt to incorporate first-principles force constants derived from *ab initio* density-functional theory (DFT) into Green's function calculation for infinitely large three-dimensional crystal structure. We also demonstrate the importance of accurate force constants by comparing the phonon transmission and thermal conductance using force constants obtained from semiempirical Stillinger-Weber potential and first-principles DFT calculations.

DOI: 10.1103/PhysRevB.86.235304 PACS number(s): 63.20.dk, 68.35.Ct, 73.40.−c, 68.35.Ja

I. INTRODUCTION

The reduced lattice thermal conductivity observed in many nanostructured materials has significant implications for applications from thermoelectric energy conversion to microelectronics thermal management. The Boltzmann transport equation (BTE) can be used to accurately model the phonon transport in nanostructures if the input parameters, such as phonon mean free paths and interfacial transmission, can be properly represented. In recent years, excellent progress has been made in computing the mode-dependent phonon mean free paths in bulk materials using first-principles approaches.[1–4] In contrast, research on phonon transmission across interfaces is still limited, and first-principles studies of phonon interfacial transport are rather scarce. First-principles-based approaches have been recently applied to nanotubes;[5,6] however, their applications to interfaces between bulk three-dimensional (3D) materials are significantly more demanding due to the large number of transverse wave vectors required.

Interface roughness due to atomic disorder and defects commonly occurs at interfaces during material synthesis. A thorough understanding of the influence of interface roughness on phonon transport is crucial for surface engineering and improved device design. It is generally accepted that interface roughness is a very important driving mechanism for thermal conductivity reduction in different nanostructures such as nanowires and superlattices. However, it is not clear how interface roughness affects interfacial phonon transmission. Using a lattice Green's function formalism, Fagas *et al.*[7] found that the phonon transmittance is strongly dependent on phonon frequency and the disorder correlation length by varying the atomic masses in a two-dimensional disordered atomic layer. Following the same approach, Zhao and Freund[8] studied the phonon scattering at a rough interface induced by atomic mixing between two fcc lattices and found that the transmittance is insensitive to the roughness parameters. Using molecular dynamics (MD) simulations, Sun and Murthy[9] focused on the transmittance change as the roughness thickness was increased. For long-wavelength phonons, they concluded that the transmittance is independent of roughness thickness. For midrange-wavelength phonons, the transmittance is reduced as roughness thickness increases but eventually saturates to become independent of the roughness. Nevertheless, the above studies have not drawn a comparison between the ideal and rough interface; furthermore, the conclusions were derived from empirical potentials. Using a simplified lattice dynamics model, Kechrakos[10] found that the interface conductance can be enhanced by as much as a factor of 3 for highly mismatched materials. The calculation only included one monolayer roughness and one branch mode. Stevens *et al.*[11] observed that interface mixing improved thermal transport by nearly a factor of 2 through nonequilibrium molecular dynamics (NEMD) simulations. Most recently, using NEMD, English *et al.*[12] found that by sandwiching an intermediate layer between two dissimilar materials, the interfacial thermal conductance can be enhanced compared to that of the two dissimilar materials. NEMD, however, is unable to unveil any information about the mode-dependent transmission. Additionally, an empirical potential was used in their simulations. The behavior of different phonon modes at a rough interface using reliably accurate force constants would be preferable, and as we show in this paper, results can differ by up to 50%, depending on the choice of the force field.

Phonon interface transmittance is critical in determining the interfacial thermal resistance. Phonon interface transmittance models have yet to reliably predict experimental observations. There are two widely used models for the phonon transmittance at an interface: the acoustic mismatch model (AMM)[13] and the diffuse mismatch model (DMM).[14] As a continuum model, the AMM assumes that phonons undergo specular reflection or transmission at the interface. This model is valid in the long-wavelength limit, where due to their small details compared to the incident phonon wavelength, interfaces are seen as sharp. The DMM, on the other hand, assumes not only purely diffuse scattering at the interface, but also an equivalence between phonon reflectance from one side to the transmittance from the other. This model, as opposed to AMM, is valid for very rough or dirty interfaces and short-wavelength phonons. Neither AMM

nor DMM consistently predict interface thermal boundary resistance. Using molecular dynamics,[9,15–19] phonon wave packets can be created and the phonon transmittance can be obtained by tracking the energy transmitted and reflected after encountering an interface. Although easy to implement, it is computationally expensive since one separate MD simulation is needed for every incoming phonon mode, although using the multiple phonon wave packets reduces computational intensity.[16] Additionally, MD simulations cannot capture a wide angle of incidence because they require a large lateral size that is difficult to achieve. Linear lattice dynamics (LD) calculations[20–23] have been performed to extract the mode-dependent phonon transmittance by solving the reflected and transmitted wave functions subject to boundary conditions. However, this method can be difficult to implement for complex atomic structures. As an alternative and more straightforward approach, Green's function methods dedicated to solve for the response from point-source perturbation are employed to compute the phonon-transmission function that can be easily related to transmittance, as described in Sec. II. The Green's function approach has been described thoroughly for transmission function calculation in electron transport by Datta.[24] Mingo and Yang[25,26] applied the approach to deal with phonon transport within an elastic scattering domain in nanowires and referred to this method as the atomistic Green's function (AGF). Later, Zhang *et al.*[27] extended the method to phonon transport in 3D structures. They calculated the phonon transmission across the Si-Ge interface using an empirical interatomic potential and investigated the strain effect on interfacial transport. A general formulation and full derivation have been detailed by Mingo and Zhang[25,26] and Zhang *et al.*[27,28] Several other studies utilize the same framework,[5,6,30–32] including the only first-principles-based calculations with the AGF method in one-dimensional (1D) structures.[5,6] Here we incorporate the first-principles force constants into AGF and demonstrate the importance of using accurate force constants. Without any fitting to experimental data, the force constants from first-principles calculations demonstrated the ability to accurately reproduce the lattice thermal conductivity of bulk materials.[1–4,33] These force constants can also improve the quantitative prediction for interfacial phonon transport. In this study, we employ the AGF method to study the interface roughness stemming from atomic mixing between Si and Ge interfaces.

II. METHODOLOGY

The detailed methodology of AGF has been presented elsewhere.[25–30] In short, the system is partitioned into three regions: the left lead, the central region (also known as the scattering region), and the right lead, as shown in Fig. 1. The advantage of Green's function lies in its ability to replace the infinite leads by finite leads with self-energies.[24] The self-energy Σ_α describes the effect of the lead α on the central block and is defined as

$$\Sigma_\alpha = \phi_{C\alpha} g_\alpha \phi_{C\alpha}^{+}, \tag{1}$$

where α stands for left (L) or right (R), C stands for center; ϕ's are the harmonic force constant matrices divided by corresponding atomic masses: ϕ_α means the onsite force constants of a block in lead α, $\phi_{\alpha\alpha}$ means the hopping matrices between two neighboring blocks within lead α; ϕ^{+} is the complex conjugate of ϕ; and g is the surface Green's function defined by

$$g_\alpha = [\omega^2 I - \phi_\alpha - \phi_{\alpha\alpha} g_\alpha \phi_{\alpha\alpha}^{+}]^{-1}. \tag{2}$$

The surface Green's function corresponds to the uncoupled semi-infinite system and is solved iteratively using a fast algorithm.[34] The coupled Green's function for the central region is expressed as

$$G^R = [\omega^2 I - \phi_C - \Sigma_L - \Sigma_R]^{-1}, \tag{3}$$

where the superscript R stands for retarded, ω is phonon frequency, and ϕ_C represents the onsite force constants of the central region.

To tackle the infinitely large size of transverse direction, a Fourier transform is performed parallel to the interface to decouple the infinite degrees of freedom into independent transverse wave vectors $\vec{k}_t$, assuming ideal translational invariance. We can then treat them as independent 1D chains with different transverse wave vectors. The transmission function $\Xi(\omega,\vec{k}_t)$ as a function of the phonon frequency and transverse wave vector is given as a trace over the Green's function of the center and coupling terms between the leads and the center:

$$\Xi(\omega,\vec{k}_t) = Tr[\Gamma_L(\omega,\vec{k}_t) G^R(\omega,\vec{k}_t) \Gamma_R(\omega,\vec{k}_t) G^A(\omega,\vec{k}_t)], \tag{4}$$

where $\Gamma_\alpha = i[\Sigma_\alpha^R - \Sigma_\alpha^A]$ describes the rate at which phonons enter and exit the leads. The retarded Green's function G^R and retarded self-energy Σ^R are the Hermitian conjugate of advanced Green's function G^A and advanced self-energy Σ^A, respectively. The total transmission at a given frequency is simply the sum of the transmission function of different transverse wave vectors normalized by the total number of transverse k points: $\Xi(\omega) = 1/N_{\vec{k}_t} \sum_{\vec{k}_t} \Xi(\omega,\vec{k}_t)$. While the phonon frequency and transverse wave vector are conserved, mode conversion is allowed and the longitudinal wave vector can change. In other words, the phonons can elastically scatter into different directions at rough interfaces.

The thermal conductance per unit area σ, based on the total transmission function $\Xi(\omega)$, is calculated using Landauer's formula,[35]

$$\sigma(T) = \frac{1}{s} \times \frac{1}{2\pi} \int_0^\infty \hbar\omega \frac{\partial f(\omega,T)}{\partial T} \Xi(\omega) d\omega, \tag{5a}$$

where f is the Bose-Einstein distribution and s is the cross-sectional area of the simulation cell perpendicular to the direction of heat flow. Note that this definition yields a finite thermal conductance in the limit of an identical material because the temperature drops ΔT used to derive Eq. (5a) are between the reservoir temperatures T_1 and T_2, instead of the temperature drop across the interface. In other words, Eq. (5a) is the formula corresponding to a two-probe setup where the thermometer probes the bulk phonons incident on the interface.[13] If a thermometer probes the temperature drop right across the interface (this corresponds to a four-probe setup), Eq. (5a) needs to be modified.[36,37] Despite highly nonequilibrium distribution near the interface, we can define equivalent

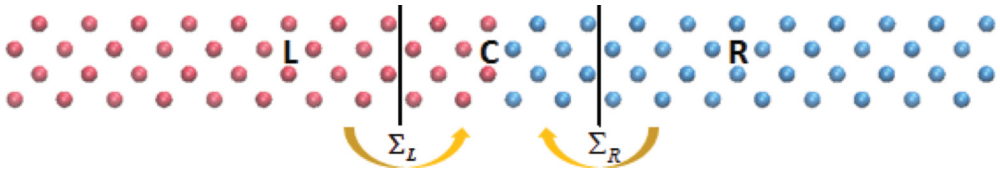

FIG. 1. (Color online) The system is divided into three parts: left (L), center (C), and right (R). Left and right leads are semi-infinite crystal lattices. In the transverse direction, all the three regions have periodic boundary conditions imposed to represent the infinitely large lateral dimension.

equilibrium temperatures T_{e1} and T_{e2} as proposed by Chen.[37] The equivalent equilibrium temperature corresponds to the final equilibrium temperature of these phonons if we assume they adiabatically approach equilibrium. Then we could use Bose-Einstein distribution as a function of the equivalent equilibrium temperature to represent the local energy density. On the other hand, we can express the local energy density as a summation of the phonons emitted from both ends with the reservoir temperatures. By equating the local energy densities from these two approaches, we obtain the relation between the equivalent equilibrium temperature and the heat reservoir temperature as $T_{e1} = T_1 + (T_2 - T_1)\sigma/(2\sigma_1)$ and $T_{e2} = T_2 - (T_2 - T_1)\sigma/(2\sigma_2)$. Finally, we reach a modified expression for the thermal conductance as

$$\sigma'(T) = \sigma(T) \times \frac{1}{1 - \frac{1}{2}\left[\frac{\sigma(T)}{\sigma_1(T)} + \frac{\sigma(T)}{\sigma_2(T)}\right]}, \tag{5b}$$

where σ_1 and σ_2 are the "thermal conductance" of pure material 1 and pure material 2, respectively, using Eq. (5a) with $\Xi(\omega)$ equaling the number of phonon bands at the frequency ω. For a pure material, Eq. (5b) gives infinite thermal conductance as there is no temperature drop across the virtual interface. In the limit of low conductance ($\sigma \ll \sigma_1, \sigma \ll \sigma_2$), Eqs. (5a) and (5b) reach the same value as the denominator approaches 1. In the following discussion (Sec. III), Eq. (5b) is applied.

Transmittance can be related to transmission function as

$$\tau_{12}(\omega) = \frac{\Xi(\omega)}{\Xi_1(\omega)}, \quad \tau_{21}(\omega) = \frac{\Xi(\omega)}{\Xi_2(\omega)}, \tag{6}$$

where $\tau_{12}(\omega)$ is the transmittance from material 1 to material 2, while $\tau_{21}(\omega)$ is the transmittance from material 2 to material 1. Transmittance describes the fraction of the incident phonons of frequency ω that is transmitted. Consequently, its value lies between zero and unity. The transmission function, on the other hand, can exceed unity because it describes the number of modes transmitted at a specific frequency. The maximum value of the transmission function at a certain frequency would be the total number of phonon modes available at that frequency. Although the transmission function from either side is identical, a requirement of detailed balance, the transmittance has directional dependence.

In this study, we first construct an ideal Si/Ge interface as shown in Fig. 1 with Si on the left of the interface and Ge on the right of the interface, using the lattice constant of Si. Lattice constants for the semiempirical Stillinger-Weber (SW) potential and DFT potential for Si are $a = 5.43$ Å and $a = 5.3976$ Å, respectively. The transverse direction of all the three regions is set to be $3a \times 3a$, which has converged by comparing to the results of the $6a \times 6a$ simulation size. Periodic boundary conditions are imposed in the transverse directions. The longitudinal length of the central region is $2a$, which equals the largest thickness of rough region investigated in this study. For simplicity, we use the force constants obtained from Si throughout the system as those of Ge are very similar in magnitude. The major factor affecting the phonons of Si and Ge are their very different masses. The atomic masses for Si and Ge are 28.085 5 and 72.63, respectively. To obtain the force constants from the SW potential and DFT, LAMMPS[38] and QUANTUM ESPRESSO[39] are used to record the force and displacement data, respectively. For our DFT calculation, we use the local density approximation of Perdew and Zunger,[40] with a cutoff energy of 40 Ryd and $4 \times 4 \times 4$ k points for a $2 \times 2 \times 2$ supercell of 64 atoms. By fitting the general expression of the Taylor expansion of the interatomic potential to the set of force displacements obtained from different atomic configurations,[41] we extract the harmonic force constants that are input into our transmission calculation. We take exactly the same parameters as Esfarjani *et al.*[1] used, where they obtained excellent agreement with experimental data for the phonon dispersion and thermal conductivity of Si. This gives us confidence on the DFT force constants and corresponding phonon properties. The harmonic force constants that determine the phonon frequencies and eigenvectors are essential for the transmission and thermal conductance. To calculate the total transmission, the number of transverse k points within the Brillouin zone is chosen to be 10×10 to ensure the convergence. A similar procedure has been followed for rough interfaces, except for the system setup that obtains the force constants. For rough interfaces, the atoms in the interface region are assigned one of the two atomic masses according to some probability (uniform or Gaussian), constrained by the thickness of the rough region, and then the effective force constants ϕ were obtained by dividing the Si force constants by the newly assigned masses. Lattice mismatch between Si and Ge, i.e., strain effects, and anharmonicity are not included in this study. As observed by the NEMD simulations,[42] anharmonic effects were not important for temperatures lower than 500 K.

To first validate our methodology, we compare our calculated thermal conductance of an ideal Si/Ge interface using SW potential and Eq. (5a) with available data in the literature. Our result yields 2.8×10^8 W/m^2 K at 300 K, which is close to 3.1×10^8 W/m^2 K from lattice dynamics calculation by Zhao and Freund,[22] and $(3.2 \pm 0.2) \times 10^8$ W/m^2 K from NEMD calculation by Landry and McGaughey.[42] We can then focus on the discussion on rough interfaces using Eq. (5b).

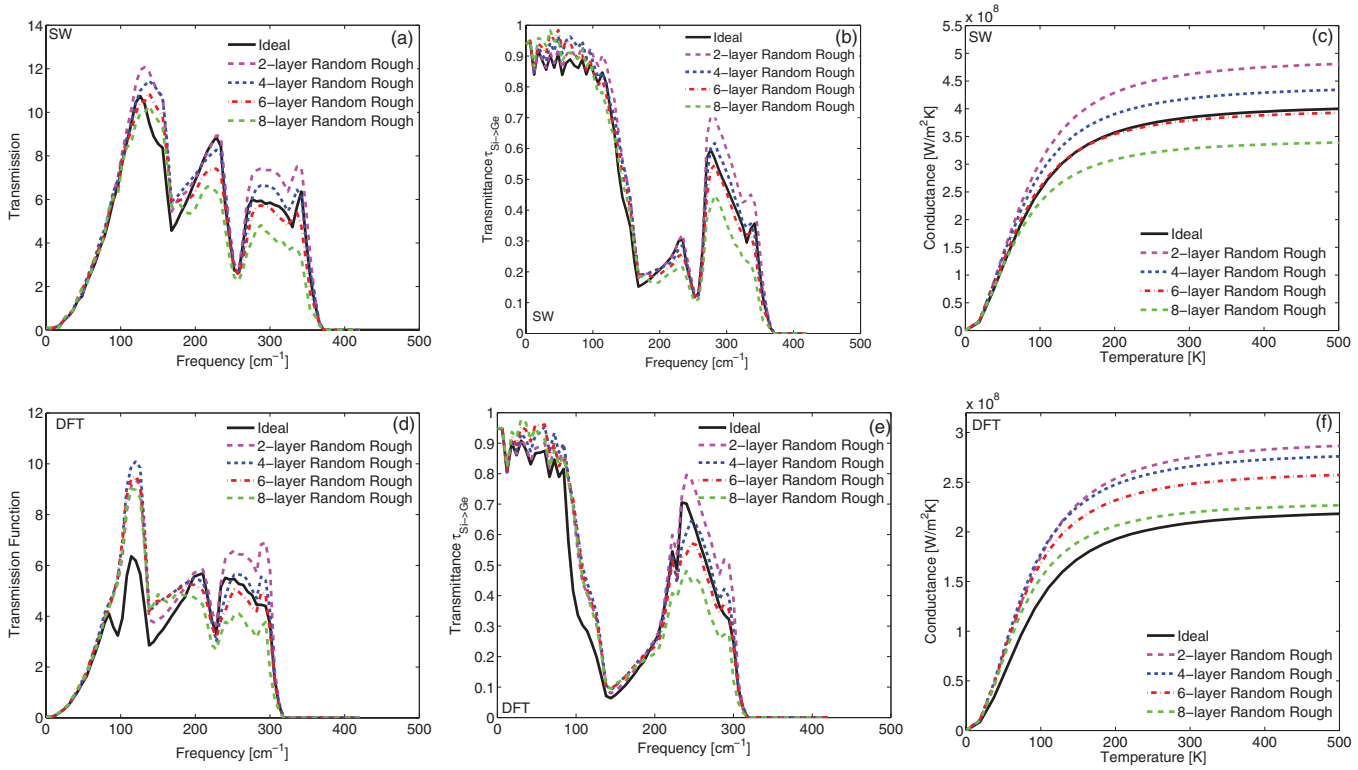

FIG. 2. (Color online) Total transmission function, transmittance, and thermal conductance as a function of phonon frequency for an ideal Si/Ge interface (solid black line) and for a random rough Si/Ge interface (colored dashed or dotted lines): (a) total transmission based on SW force constants; (b) transmittance from Si to Ge based on SW force constants; (c) thermal conductance based on SW force constants; (d) total transmission based on DFT force constants; (e) transmittance from Si to Ge based on DFT force constants; and (f) thermal conductance based on DFT force constants.

III. RESULTS AND DISCUSSION

A. Rough interface with random distribution

To create random atomic mixing, we select a certain number of layers (2, 4, 6, and 8) in the central region and randomly shuffle the atoms within these layers. Three independent configurations are constructed for each roughness thickness, and calculations are conducted for each configuration. The average value is plotted for each thickness of the rough region. The total transmission function, transmittance, and thermal conductance are plotted in Fig. 2. The total transmission function, transmittance, and thermal conductance of ideal interface are plotted in Fig. 2 as a reference.

One counterintuitive finding, arguably the most important highlight, from Fig. 2 is that the phonon transmission across a rough Si/Ge interface can be higher than the ideal Si/Ge interface for certain frequencies, contributing to a larger thermal conductance at certain roughness thicknesses. In the low-frequency limit, the long-wavelength phonons do not sense the interface roughness and propagate through as if they are traveling across the ideal sharp interface. Due to its short length scale, atomic roughness has negligible influence on the long-wavelength phonons. In the high-frequency limit, the transmission is zero because there are no available states on the Ge side. The most interesting phenomena are observed for the phonons with midrange frequencies, where the atomic roughness could play a role in enhancing the transmission. The roughness softens the abrupt change of acoustic impedance at the interface and facilitates phonon propagation. It can also allow phonons with large incidence angles, which would otherwise be internally reflected at the interface, to be transmitted. More specifically, this can be understood by investigating the phonon density of states (DoS) of the two materials, where incident and outgoing phonons are contained, and the interfacial region where reflection and transmission happens. As shown in Fig. 3, the phonon DoS of pure Si and Ge are quite different, while the Si/Ge mixture has intermediate DoS, which serve to bridge the gap between Si and Ge. Therefore, phonons that originally cannot propagate across the Si/Ge interface can now transmit via new elastic scattering channels created in the Si/Ge mixture. Accordingly, the phonon transmission and transmittance are boosted in the 200–300 cm^{-1} frequency range where the overlap of the two DoS is enhanced. This frequency range corresponds to the top of the transverse acoustic branches close to the zone boundary, where the typical phonon wavelength is a few lattice constants at the most. Although one configuration of a Si/Ge mixture is used in Fig. 3, it can represent the trend of general Si/Ge mixtures at the interface, since the atomic ratio of all the configurations involved in our calculation is 1:1, with the only difference being atomic positions. In fact, it has been well known that interface roughness can

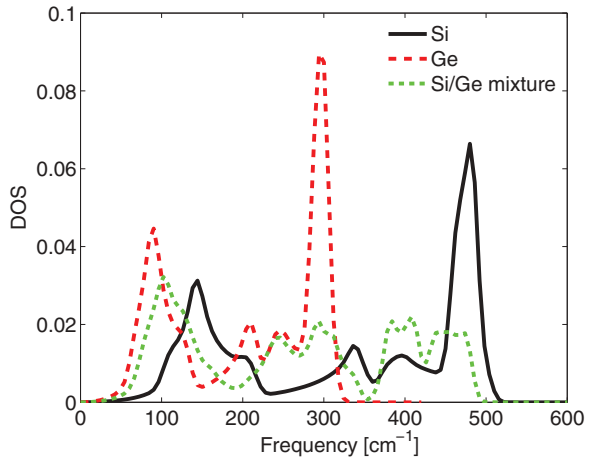

FIG. 3. (Color online) Phonon density of states (DoS) of pure Si (black solid line), pure Ge (red dashed line), and Si/Ge 1:1 mixture (green dotted line) using DFT force constants.

increase transmittance of photons[43–46] and electrons.[47–50] For phonons, interface roughness leads to reduction in thermal conductivity in nanowires[51–53] because of backscattering and in superlattices[54–56] due to loss of coherence, but for an individual interface, interface roughness is able to increase transmittance. This has not received much attention before.

For the two-layer rough configuration, SW predicts an ∼20% increase in the thermal conductance at 300 K, while DFT predicts a ∼30% increase, compared to perfect interfaces. Empirical potentials can qualitatively capture the trend but are unable to quantitatively predict the difference. As the thickness of the rough region increases, the transmission does not keep increasing, which is consistent with earlier observations.[9,12] There are two competing factors: (1) overlapping DoS which increases transmission and (2) diffuse scattering at the rough interface, which reduces transmission. As observed in the SW case [Fig. 2(a)], the two-layer rough configuration gives the highest transmission. Above a thickness of two layers, diffuse scattering becomes the more significant mechanism that affects thermal conductance. In the DFT case [Fig. 2(d)], however, the four-layer rough configuration gives the highest transmission around 120 cm^{-1}, and the two-layer roughness gives the highest transmission between 230 and 300 cm^{-1}, which leads to fairly close thermal conductance between the two-layer rough configuration and the four-layer rough configuration, as shown in Fig. 2(f). This finding cannot be represented by the calculation using SW prediction, partly because their phonon bandwidths are different from DFT. Compared to the ideal interface, the thermal conductance is larger when the rough region is thinner than six layers using SW force constants and up to eight layers using DFT force constants. This discrepancy reiterates the necessity of adopting DFT force constants to provide precise guidance in practical applications. In the following discussion, only DFT force constant results are presented. As thickness increases even further, the thermal conductance decreases below that of the ideal interface. This can be easily understood by considering the limiting case. As the thickness of the rough region increases to infinity, diffuse scattering becomes dominant and the thermal conductance should approach the alloy limit.

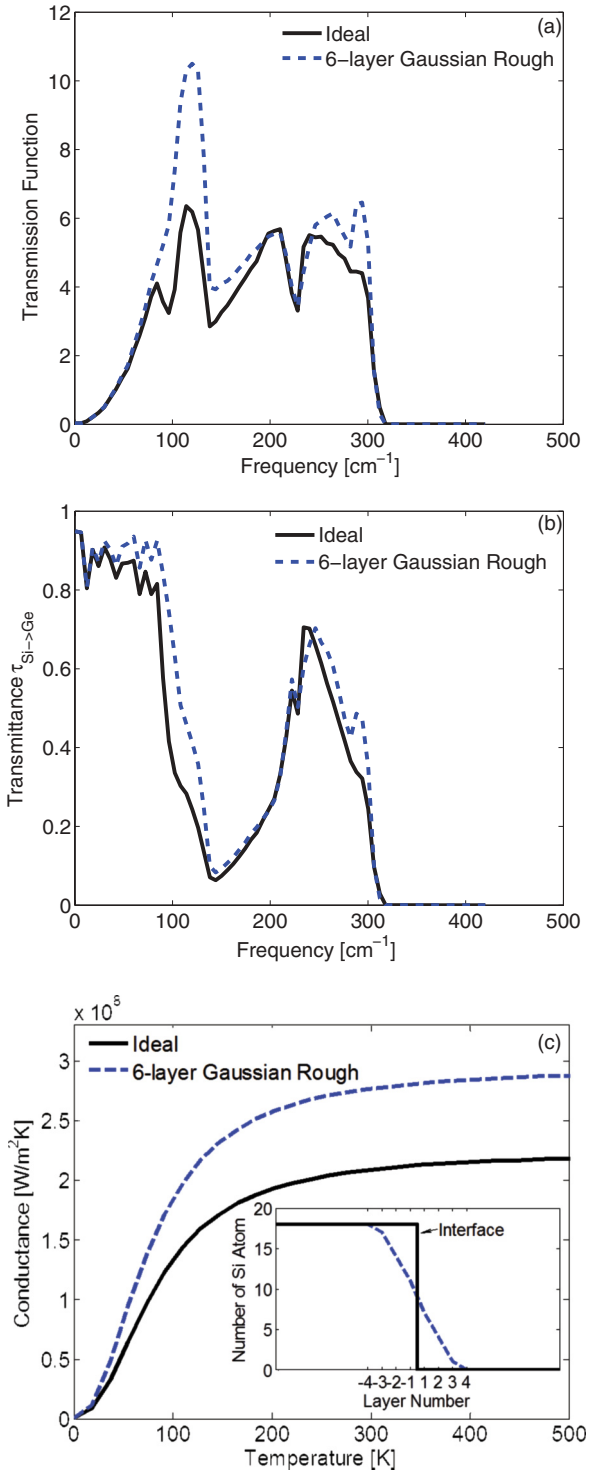

FIG. 4. (Color online) (a) Total transmission function, (b) transmittance, and (c) thermal conductance as a function of phonon frequency for an ideal Si/Ge interface (solid black line) and for a rough Si/Ge interface with a Gaussian distribution (dashed blue lines) based on DFT force constants. (c, Inset) The number of Si atoms in each layer for an ideal interface (solid black) and for a Gaussian rough interface (dashed blue).

B. Rough interface with Gaussian distribution

To mimic atomic diffusion at an interface, we also create the atomic profile of one type to obey half-Gaussian distribution,

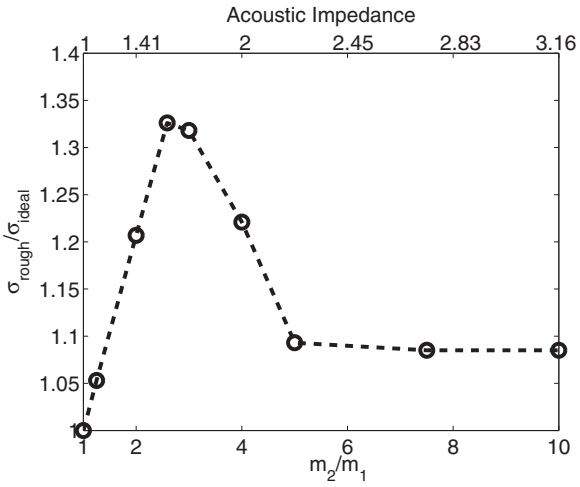

FIG. 5. Thermal conductance ratio of a Gaussian rough interface to an ideal interface as a function of the mass ratio (lower x axis) and the acoustic impedance ratio (upper x axis) of the two materials using DFT force constants

as shown in the Fig. 4(c) inset. The phonon transmission, phonon transmittance, and thermal conductance are plotted in Fig. 4. A significant increase in phonon transmission is observed using DFT force constants. At 300 K, there is a 32.6% increase. For the same roughness thickness, the Gaussian distribution shows more enhanced transmission compared to the uniform roughness distribution.

Comparison with experimental data is difficult since there is no experimental data on a single Si/Ge interface. On the other hand, several experiments had reported reduced thermal conductivity on Si/Ge superlattices.[54,55] If we assume that the measured thermal conductivity is due to interfacial resistances only, as one would expect in the very thin limit when phonon transport is completely incoherent[57] and yet ballistic through individual layers of the superlattice, the extrapolated thermal conductance is 2×10^9 W/m^2 K[54] (period = 3 nm) and 1.8×10^9 W/m^2 K [55] (period = 4.4 nm) at 300 K. Both the extrapolated values are close but about 1 order of magnitude larger than our calculated value of 2.8×10^8 W/m^2 K for an ideal interface and 2.8×10^8 W/m^2 K for a Gaussian rough interface based on DFT force constants. The higher-than-predicted value is actually consistent with recent experimental observation[58] that long-wavelength phonons maintain their coherence in thermal transport in superlattices, and hence lead to a higher conductance value than that of a single interface as we calculated.

To explore the generality of the transmission enhancement between different materials, we keep the Gaussian rough configuration and vary the mass of the atoms on the Ge sites from 1.25 times that of Si to ten times that of Si, corresponding to acoustic mismatch from 1 to 3.16. The thermal conductance ratio of a Gaussian interface over an ideal interface is plotted in Fig. 5 as a function of the mass/acoustic impedance ratio of the two materials on both sides of the interface. Since the roughness is caused by the mass difference, when the mass ratio is 1, there is no atomic mixing and no roughness. As the mass ratio increases, the phonon dispersions of the two materials begin to differ from each other and the roughness favors phonon propagation via graded acoustic impedances at the interface. The thermal conductance ratio reaches its maximum at 2.586, which happens to be the mass ratio of Si to Ge. As the mass ratio increases even further, the phonon dispersions of two materials fall further apart from each other and it becomes less effective to bridge the large gap through the effects of roughness. Therefore, the thermal conductance ratio drops and flattens out with increasing mass ratio. Nevertheless, the thermal conductance ratio is kept over unity up to a mass ratio of 10 and will stay above unity in the infinite mass mismatch limit, as it provides a smooth transition for intermediate-frequency phonons to transmit across the interface. Although there are variations in the extent to which roughness increases thermal conductance, the enhancement generally holds.

IV. CONCLUSION

In summary, we apply the atomistic Green's function method to calculate the phonon transmission across an ideal and rough Si/Ge interface. The atomistic roughness can increase phonon transmission across two dissimilar materials if the roughness thickness and profile are properly controlled, contrary to the commonly held notion that rougheness reduces transmission. This effect is more pronounced if the acoustic mismatch between the two materials is moderately large. This finding elucidates new design considerations for surface engineering. As our contribution to the AGF framework, we incorporate the first-principles force constants determined from DFT into the AGF method for phonon transport in infinitely large 3D structure. The comparison between the results from SW force constants and those from DFT force constants demonstrates that DFT force constants are necessary in reliable predictions. Since interface transmission is crucial for bridging the calculation of pure materials to nanocomposites, we can now integrate the interfacial transmission and the bulk mean free paths, both calculated from first-principles DFT, to accurately model heat transport in complex nanostructured materials.

ACKNOWLEDGMENTS

This material is based upon work supported as part of the S3TEC, an Energy Frontier Research Center funded by the US Department of Energy, Office of Science, Office of Basic Energy Sciences, under Award No. DE-FG02-09ER46577.

*gchen2@mit.edu

[1] K. Esfarjani, G. Chen, and H. T. Stokes, Phys. Rev. B **84**, 085204 (2011).

[2] J. Shiomi, K. Esfarjani, and G. Chen, Phys. Rev. B **84**, 104302 (2011).

[3] T. Shiga, J. Shiomi, J. Ma, O. Delaire, T. Radzynski, A. Lusakowski, K. Esfarjani, and G. Chen, Phys. Rev. B **85**, 155203 (2012).

[4] Z. Tian, J. Garg, K. Esfarjani, T. Shiga, J. Shiomi, and G. Chen, Phys. Rev. B **85**, 184303 (2012).

[5]N. Mingo, D. A. Stewart, D. A. Broido, and D. Srivastava, Phys. Rev. B **77**, 033418 (2008).
[6]D. Stewart, I. Savic, and N. Mingo, Nano Lett. **9**, 81 (2009).
[7]G. Fagas, A. G. Kozorezov, C. J. Lambert, J. K. Wigmore, A. Peacock, A. Poelaert, and R. den Hartog, Phys. Rev. B **60**, 6459 (1999).
[8]H. Zhao and J. Freund, J. Appl. Phys. **105**, 013515 (2009).
[9]L. Sun and J. Murthy, Trans. ASME: J. Heat Transfer **132**, 102403 (2010).
[10]D. Kechrakos, J. Phys.: Condens. Matter **3**, 1443 (1991).
[11]R. J. Stevens, L. V. Zhigilei, and P. M. Norris, Int. J. Heat Mass Transf. **50**, 3977 (2007).
[12]T. S. English, J. C. Duda, J. L. Smoyer, D. A. Jordan, P. M. Norris, and L. V. Zhigilei, Phys. Rev. B **85**, 035438 (2012).
[13]W. Little, Can. J. Phys. **37**, 334 (1959).
[14]E. Swartz and R. Pohl, Rev. Mod. Phys. **61**, 605 (1989).
[15]P. Schelling, S. Phillpot, and P. Keblinski, Appl. Phys. Lett. **80**, 2484 (2002).
[16]C. Kimmer, S. Aubry, A. Skye, and P. K. Schelling, Phys. Rev. B **75**, 144105 (2007).
[17]P. Schelling and S. Phillpot, J. Appl. Phys. **93**, 5377 (2003).
[18]Z. T. Tian, B. E. White, and Y. Sun, Appl. Phys. Lett. **96**, 263113 (2010).
[19]N. Zuckerman and J. R. Lukes, Phys. Rev. B **77**, 094302 (2008).
[20]D. A. Young and H. J. Maris, Phys. Rev. B **40**, 3685 (1989).
[21]S. Pettersson and G. D. Mahan, Phys. Rev. B **42**, 7386 (1990).
[22]H. Zhao and J. Freund, J. Appl. Phys. **97**, 024903 (2005).
[23]J. Wang and J. S. Wang, Phys. Rev. B **74**, 054303 (2006).
[24]S. Datta, *Electronic Transport in Mesoscopic Systems* (Cambridge University Press, Cambridge, UK, 1997).
[25]N. Mingo and L. Yang, Phys. Rev. B **68**, 245406 (2003).
[26]N. Mingo and L. Yang, Phys. Rev. B **70**, 249901(E) (2004).
[27]W. Zhang, T. Fisher, and N. Mingo, Trans. ASME: J. Heat Transfer **129**, 483 (2007).
[28]W. Zhang, T. Fisher, and N. Mingo, Numer. Heat Transfer, Part B **51**, 333 (2007).
[29]S. Volz, Thermal Nanosystems and Nanomaterials **118**, 1 (2009).
[30]A. Dhar and D. Roy, J. Stat. Phys. **125**, 805 (2006).
[31]P. Hopkins, P. Norris, M. Tsegaye, and A. Ghosh, J. Appl. Phys. **106**, 063503 (2009).
[32]X. Li and R. Yang, Phys. Rev. B **86**, 054305 (2012).
[33]D. Broido, M. Malorny, G. Birner, N. Mingo, and D. Stewart, Appl. Phys. Lett. **91**, 231922 (2007).
[34]M. P. López Sancho, J. M. López Sancho, and J. Rubio, J. Phys. F **15**, 851 (1985).
[35]R. Landauer, Philos. Mag. **21**, 863 (1970).
[36]J. A. Katerberg, C. L. Reynolds, and A. C. Anderson, Phys. Rev. B **16**, 673 (1977).
[37]G. Chen, *Nanoscale Energy Transport and Conversion: A Parallel Treatment of Electrons, Molecules, Phonons, and Photons* (Oxford University Press, New York, 2005).
[38]S. Plimpton, J. Comput. Phys. **117**, 1 (1995).
[39]P. Giannozzi, S. Baroni, N. Bonini, M. Calandra, R. Car, C. Cavazzoni, D. Ceresoli, G. L. Chiarotti, M. Cococcioni, I. Dabo, A. Dal Corso, S. Fabris, G. Fratesi, S. de Gironcoli, R. Gebauer, U. Gerstmann, C. Gougoussis, A. Kokalj, M. Lazzeri, L. Martin-Samos, N. Marzari, F. Mauri, R. Mazzarello, S. Paolini, A. Pasquarello, L. Paulatto, C. Sbraccia, S. Scandolo, G. Sclauzero, A. P. Seitsonen, A. Smogunov, P. Umari, and R. M. Wentzcovitch, J. Phys.: Condens. Matter **21**, 395502 (2009).
[40]J. P. Perdew and A. Zunger, Phys. Rev. B **23**, 5048 (1981).
[41]K. Esfarjani and H. T. Stokes, Phys. Rev. B **77**, 144112 (2008).
[42]E. S. Landry and A. J. H. McGaughey, Phys. Rev. B **80**, 165304 (2009).
[43]Y. Kanamori, M. Sasaki, and K. Hane, Opt. Lett. **24**, 1422 (1999).
[44]Y. F. Huang, S. Chattopadhyay, Y. J. Jen, C. Y. Peng, T. A. Liu, Y. K. Hsu, C. L. Pan, H. C. Lo, C. H. Hsu, Y. H. Chang, C. S. Lee, K. H. Chen, and L. C. Chen, Nat. Nanotechnol. **2**, 770 (2007).
[45]K. Choi, S. H. Park, Y. M. Song, Y. T. Lee, C. K. Hwangbo, H. Yang, and H. S. Lee, Adv. Mater. **22**, 3713 (2010).
[46]K. C. Park, H. J. Choi, C. H. Chang, R. E. Cohen, G. H. McKinley, and G. Barbastathis, ACS Nano **6**, 3789 (2012).
[47]K. Tai, L. Yang, Y. Wang, J. Wynn, and A. Cho, Appl. Phys. Lett. **56**, 2496 (1990).
[48]M. Peters, B. Thibeault, D. Young, J. Scott, F. Peters, A. Gossard, and L. Coldren, Appl. Phys. Lett. **63**, 3411 (1993).
[49]M. Hong, J. Mannaerts, J. Hong, R. Fischer, K. Tai, J. Kwo, J. Vandenberg, Y. Wang, and J. Gamelin, J. Cryst. Growth **111**, 1071 (1991).
[50]S. Chalmers, K. Lear, and K. Killeen, Appl. Phys. Lett. **62**, 1585 (1993).
[51]D. Y. Li, Y. Y. Wu, P. Kim, L. Shi, P. D. Yang, and A. Majumdar, Appl. Phys. Lett. **83**, 2934 (2003).
[52]A. I. Hochbaum, R. K. Chen, R. D. Delgado, W. J. Liang, E. C. Garnett, M. Najarian, A. Majumdar, and P. D. Yang, Nature (London) **451**, 163 (2008).
[53]A. I. Boukai, Y. Bunimovich, J. Tahir-Kheli, J. K. Yu, W. A. Goddard, and J. R. Heath, Nature (London) **451**, 168 (2008).
[54]S. M. Lee, D. G. Cahill, and R. Venkatasubramanian, Appl. Phys. Lett. **70**, 2957 (1997).
[55]T. Borca-Tasciuc, W. L. Liu, J. L. Liu, T. F. Zeng, D. W. Song, C. D. Moore, G. Chen, K. L. Wang, M. S. Goorsky, T. Radetic, R. Gronsky, T. Koga, and M. S. Dresselhaus, Superlattices Microstruct. **28**, 199 (2000).
[56]E. S. Landry and A. J. H. McGaughey, Phys. Rev. B **79**, 075316 (2009).
[57]G. Chen, Phys. Rev. B **57**, 14958 (1998).
[58]M. N. Luckyanova, J. Garg, K. Esfarjani, A. Jandl, M. T. Bulsara, A. J. Schmidt, A. J. Minnich, S. Chen, M. S. Dresselhaus, Z. Ren, E. A. Fitzgerald, and G. Chen, Science **338**, 936 (2012).